Supplementary Figures, Tables and Methods

Supplementary Materials for

microRNA regulation of persistent stress-enhanced memory

Authors: Stephanie E. Sillivan[1, 2], Sarah Jamieson[1, 2], Laurence de Nijs[3], Meghan Jones[1, 2], Clara Snijders[3], Torsten Klengel[4], Nadine F. Joseph[1,2], Julian Krauskopf[5], Jos Kleinjans[5], Christiaan H. Vinkers[6], Marco P.M. Boks[6], Elbert Geuze[6,7], Eric Vermetten[6,7,8], Kerry J. Ressler[4], Bart P.F. Rutten[3], Gavin Rumbaugh[2] and Courtney A. Miller[1, 2]*

Affiliations:
[1]Department of Molecular Medicine, The Scripps Research Institute, Jupiter, FL USA

[2]Department of Neuroscience, The Scripps Research Institute, Jupiter, FL USA.

[3]School for Mental Health and Neuroscience, Department of Psychiatry and Neuropsychology, Maastricht University, Maastricht, The Netherlands.

[4]Division of Depression and Anxiety Disorders, Department of Psychiatry, Harvard Medical School, McLean Hospital, Belmont, MA, USA.

[5]Department of Toxicogenomics, Maastricht University, Maastricht, The Netherlands.

[6]Brain Center Rudolf Magnus, Department of Psychiatry, University Medical Center Utrecht, The Netherlands.

[7]Research Centre for Military Mental Healthcare, Ministry of Defence, Utrecht, The Netherlands.

[8]Department of Psychiatry, Leiden University Medical Center, Leiden, The Netherlands.

*Correspondence to: cmiller@scripps.edu.

This PDF file includes:

Materials and Methods

Animals: Adult C57BL/6 mice, 8-10 weeks of age (The Jackson Laboratory, Bar Harbor, ME), were maintained on a 12:12 hour light/dark cycle and supplied with food and water ad libitum.

Mice were group housed 3-4/cage, acclimated to the facility for 1 week then handled for 3 days prior to experiments. Behavioral tests were performed between 8AM and 5PM. Treatment groups were randomized for all behavioral experiments to prevent batch effects due to time of day. All procedures were performed in accordance with the Institutional Animal Care and Use Committee (IACUC) at the Scripps Florida Research Institute and with national regulations and policies.

Stress-enhanced fear learning (SEFL): Acute restraint stress and auditory fear conditioning were performed as previously described (Sillivan, Joseph et al. 2017) to produce stress susceptible (SS) and stress resilient (SR) populations of male animals. Briefly, animals were restrained for 2 hours and 7 days later underwent two 10Khz tone-shock pairings (0.5mA, 1 second). Classification of animals into SS/SR subpopulations was based on freezing during the last 60 seconds of shock training, which we have previously demonstrated to correlate with long term extinction resistance and fear memory expression. Female mice went through the SEFL paradigm but were not separated into SS/SR subpopulations as we have previously demonstrated that female mice do not segregate (Sillivan, Joseph et al. 2017).

Behavioral Paradigms: Animals were tested for extinction with 60 tone presentations over two days (30 per day) and/or memory recall with a 5-tone recall test. Extinction and recall were both performed in a context (context B) unique from training (context A). To determine if the memory trace was still intact in SS animals after full extinction, SS mice went through an identical weak fear conditioning paradigm that began with habituation to context A for 3X4 min trials 24 hours after the 5 tone recall test (recall 1). The next day (48 hours after recall 1), mice received 2 subthreshold CS-US pairings at 0.15mA. 24 hours later, mice were tested in a 5 tone recall test in context B (recall 2). For a full description of fear conditioning, extinction and anxiety tests

(open field, elevated plus maze [EPM] and acoustic startle response), please refer to previously described descriptions (Sillivan, Joseph et al. 2017).

Human serum samples: All subjects (N = 24) were part of a large prospective cohort study of 1,032 Dutch military soldiers that were deployed to Afghanistan between 2005 and 2009 for a period of four months. Based on the level of combat trauma exposure during deployment and the severity of PTSD symptoms, three subgroups were identified as previously described (refer to Rutten et al. Mol. Psychiatry 2017); (1) susceptible individuals, i.e. trauma-exposed soldiers with deployment-related PTSD symptoms at 6 months follow-up, (2) resilient individuals, i.e. trauma-exposed soldiers without PTSD at follow-up, and (3) controls, i.e. non-exposed and mentally healthy soldiers. Six months following the deployment period, blood samples were collected at the University Medical Centre Utrecht (Utrecht, the Netherlands) and processed to serum using standard protocol (van Zuiden, Geuze et al. 2011). Following the deployment period, trauma exposure was assessed using a 19-item deployment experiences checklist (van Zuiden, Geuze et al. 2011) and the severity of PTSD symptoms was established using the 22-item Self-Rating Inventory for PTSD (SRIP) (Hovens, Bramsen et al. 2002). All participants gave written informed consent and the study was conducted in accordance with the Declaration of Helsinki.

Human brain tissue: Human amygdala containing all major sub-nuclei was dissected, snap frozen and stored at -80°C until further processing. Tissue was isolated from four control post-mortem brain samples (details below) from the Harvard Brain and Tissue Resource Center (HBTRC) at Mclean Hospital.

Sample	Group	Sex	Age	PMI	RIN
#30	Control	F	44	10.7	7.8
#8	Control	F	61	16.8	6.7
#39	Control	M	74	14.3	5.3
#55	Control	M	57	17.3	5.1

PMI: post-mortem interval in hours; RIN: RNA integrity number

RNA and protein extraction: For rodent studies, total RNA and proteins were simultaneously extracted from fresh frozen bilateral tissue punches using the miRVANA PARIS RNA extraction kit (Life Technologies, Carlsbad, CA) following the manufacturer's instructions, as previously reported (Rumbaugh, Sillivan et al. 2015). After the initial lysis step, tissue homogenates were split into RNA or protein tubes and processed separately. 5X radioimmunoprecipitation assay buffer (RIPA, 100mM Tris-HCl [pH 7.5], 750mM NaCl, 5mM ethylenediaminetetraacetic acid [EDTA], 5mM ethylene glycol-bis[β-aminoethyl ether]-N,N,N',N'-tetraacetic acid, 5% nonyl phenoxypolyethoxylethanol, 5% sodium deoxycholate) with 5X Halt Protease and Phosphatase Inhibitor Cocktail (Thermo Scientific) was added to the protein fractions, which were sonicated, spun at 4°C for 10 min at 15,000 X g to remove cellular debris and then analyzed for yield with the Thermo Scientific bicinchoninic acid (BCA) Assay (Thermo Scientific). RNA concentrations were measured with a Qubit 3.0 Fluorometer and the Qubit RNA High Sensitive Assay (Invitrogen, Carlsbad, California, USA). For human expression analyses, total RNA including small RNAs was extracted using the Norgen RNA/DNA/Protein Purification Plus Kit (Norgen Biotek, Ontario, Canada) according to the manufacturers protocol.

miRNA Library Preparation, Sequencing and data analysis: smRNA-seq was performed on two biological replicate cohorts of mouse BLC samples at two distinct sequencing facilities, the Scripps Florida Genomics Core and the Genomic Sequencing Laboratory at Hudson Alpha. For sequencing at Scripps, total RNA was quantified by Qubit and run on the Agilent 2100 Bioanalyzer (Agilent Technologies, Santa Clara, CA) for quality assessment. All RNA Integrity Numbers (RINs) were > 7.0. 750ng total RNA was processed using the TruSeq small RNA library prep kit (Illumina, San Diego, CA). Briefly, RNA samples were sequentially ligated with 3' and 5' RNA adapters. The adapter ligated RNA molecules were reverse transcribed and PCR amplified. The

polymerase chain reaction (PCR) amplified products were visualized on a bioanalyzer and pooled 1:1 based on the concentration of the miRNA library peaks (migrating between 130-170bp). The pooled libraries were size selected on a 6% tris-borate EDTA gel to recover the miRNA library fragments. After gel extraction and ethanol precipitation of the DNA, the final library was quantified using Qubit and visualized on the Bioanalyzer. The library pool was loaded onto the NextSeq 500 flow cell (Illumina) at 1.8pM final concentration and sequenced with single-end 50bp sequencing to yield at least 20 million reads per sample. Reads were trimmed of adapter sequences using cutadapt (Martin 2011) with the following options: -a TGGAATTCTCGGGTGCCAAGG -O 3 -m 14 -M 25. All known hairpin and mature miRNAs were downloaded from miRbase version 21 (Griffiths-Jones 2004, Griffiths-Jones, Grocock et al. 2006, Griffiths-Jones, Saini et al. 2008, Kozomara and Griffiths-Jones 2014). miRNAs were identified using mirDeep2 (Friedlander, Mackowiak et al. 2012) against the mouse genome (GENCODE version GRCm38.p3) using mapper.pl with the following options: mapper.pl cutadapt.fastq -e -h -p mouseGENCODE -s mapped.fa -t samp.arf -m –v, followed by quantifier.pl using the options: -p precursor.fa -m mature.fa -r mapped.fa -t mmu, and finally by the miRDee2.pl wrapper script with the options: mapped.fa Genome.fasta samp.arf MaturemiRNA.fa none HairpinPrecursor.fa -t Mouse -q miRBase.mrd. Tables of counts were generated using unique combinations of the miRNA precursor and mature miRNA names and analyzed using DESeq2 (version 1.10.1, R version 3.2.3) (Love, Huber et al. 2014). For sequencing performed at Hudson Alpha, 200ng total RNA from each sample was taken into a small RNA library preparation protocol using NEBNext Small RNA Library Prep Set for Illumina (New England BioLabs Inc., Ipswich, MA, USA) according to the manufacturer's protocol. Briefly, 3` adapters were ligated to total input RNA followed by hybridization of multiplex SR reverse transcription (RT) primers and ligation of multiplex 5` SR

adapters. RT was done using ProtoScript II RT for 1 hour at 50°C. Immediately after RT reaction, PCR amplification was performed for 15 cycles using LongAmp Taq 2X master mix. Illumina indexed primers were added to uniquely barcode each sample. Post- PCR material was purified using QIAquick PCR purification kit (Qiagen Inc., Valencia, CA, USA). Post-PCR yield and concentration of the prepared libraries were assessed using Qubit and DNA 1000 chip on Agilent 2100 Bioanalyzer (Applied Biosystems, Carlsbad, CA, USA), respectively. Size selection of small RNA was done using a 3% dye free agarose gel cassette on Pippin prep instrument (Sage Science Inc., Beverly, MA, USA). Post-size selection yield and concentration of the libraries were assessed using Qubit 2.0 Fluorometer and DNA High sensitivity chip on Agilent 2100 Bioanalyzer, respectively. Accurate quantification for sequencing applications was performed using the qPCR-based KAPA Biosystems Library Quantification kit (Kapa Biosystems, Inc., Woburn, MA, USA). Each library was diluted to a final concentration of 1.25nM and pooled in equimolar ratios prior to clustering. Single End (SE) sequencing (50bp) was performed to generate at least 15 million reads per sample on an Illumina HiSeq2500 sequencer (Illumina). Post processing of the sequencing reads from miRNA-seq experiments from each sample was performed as per the Genomic Services Laboratory's unique in-house pipeline. Briefly, quality control checks on raw sequence data from each sample were performed using FastQC (Babraham Bioinformatics, London, UK). Raw reads were imported on a commercial data analysis platform AvadisNGS (Strand Scientifics, CA). Adapter trimming was done to remove ligated adapter from 3' end of the sequenced reads with only one mismatch allowed, poorly aligned 3' ends were also trimmed. Sequences shorter than 15 nucleotides length were excluded from further analysis. Trimmed Reads with low qualities (base quality score less than 30, alignment score less than 95, mapping quality less than 40) were removed. Filtered reads were then used to extract and

count the small RNA which was annotated with miRNAs from the miRBase release 20 database (Griffiths-Jones 2004, Griffiths-Jones, Grocock et al. 2006, Griffiths-Jones, Saini et al. 2008, Kozomara and Griffiths-Jones 2014). The quantification operation carries out measurement at both the gene level and at the active region level. Active region quantification considers only reads whose 5' end matches the 5' end of the mature miRNA annotation. miRNAs that had at least 0.5 $\log_2$ fold change between SS and SR in both sequencing runs were considered 'candidate miRNAs' and analyzed for pathway analysis with DIANA mirPATH software (Vlachos, Zagganas et al. 2015), which integrates information from TargetScan (Agarwal, Bell et al. 2015) to predict significant pathways of enriched target genes for a give list of miRNAs. Target prediction analysis was examined using DIANA's microCts and Tarbase algorithms as well as TargetScan. For human serum samples, total RNA was isolated from 300 µl of serum from 24 subjects (N = 8 per group) at 6 months follow-up using the mirVana™ PARIS™ kit (Ambion) according to the manufacturer's instructions. RNA concentration and quality were measured using an Agilent Technologies 2100 Bioanalyzer. Small RNA libraries were prepared using the TruSeq Small RNA-Seq Preparation Kit (Illumina) and used for high-throughput sequencing on a Genome Analyser HiSeq2000 (Illumina) according to the manufacturer's protocol. Quality control of the raw sequences was performed using the FastQC toolkit after which the reads were preprocessed using miRge to filter out the Illumina 3' and 5' adapters. Trimmed reads were then aligned to known mature miRNAs (miRBase version 21.0) to allow for identification of miRNAs. The expression output was analyzed using the open-source software R (version 3.4.0) and Bioconductor. The number of miRNAs in each sample was normalized against the total number of reads and differentially expressed miRNAs were detected using the DESeq2 package in R. Statistical

significance was reached when *p* value was below 0.05. Multiple testing adjustments were done using the Benjamini-Hochberg method.

QPCR: A cDNA library was created from 50ng of total RNA using the mirCURY LNA RT Kit (Qiagen, Germantown, MD) following the manufacturer's protocol. cDNA was diluted 1:80 for PCR. PCR reactions were performed in triplicate for each sample using the miRCURY LNA SYBR Green PCR Kit and the following locked nucleic acid (LNA) SYBR green primers from Qiagen: *hsa-miR-135b-5p,* assay ID: YP00204130; *hsa-miR-135a-5p* assay ID: YP00204762*; snord68,* assay ID: YP00203911; *snord38B,* assay ID: YP00203901. PCR cycle conditions were 95°C for ten minutes then 40 amplification cycles of 95°C for 10 seconds to denature and 60°C for 1 minute to anneal and elongate. A melt curve was run for each primer to verify the formation of only one product. Data were normalized to the housekeeping snoRNAs snord68 and snord38B using the $\Delta\Delta c_t$ method (Livak and Schmittgen 2001).

Quantitative mass spectrometry: Pooled samples from each treatment group were submitted for liquid chromatography–mass spectrometry (LC-MS) that was performed on an LTQ Orbitrap Elite (Thermo Fisher, Waltham, MA) equipped with Waters NanoAcquity HPLC pump (Milford, MA) at the Harvard Mass Spectrometry and Proteomics Resource Laboratory. Peptides were separated onto a 100 µm inner diameter microcapillary trapping column packed first with approximately 5 cm of C18 Reprosil resin (5 µm, 100 Å, Dr. Maisch GmbH, Germany) followed by analytical column ~20 cm of Reprosil resin (1.8 µm, 200 Å, Dr. Maisch GmbH, Germany). Separation was achieved through applying a gradient from 5–27% ACN in 0.1% formic acid over 90 min at 200 nl min−1. Electrospray ionization was enabled through applying a voltage of 1.8 kV using a home-made electrode junction at the end of the microcapillary column and sprayed from fused silica pico tips (New Objective, MA). The LTQ Orbitrap Elite was operated

in data-dependent mode for the mass spectrometry methods. The mass spectrometry survey scan was performed in the Orbitrap in the range of 395 –1,800 m/z at a resolution of 6 × 104, followed by the selection of the twenty most intense ions (TOP20) for CID-MS2 fragmentation in the Ion trap using a precursor isolation width window of 2 m/z, AGC setting of 10,000, and a maximum ion accumulation of 200 ms. Singly charged ion species were not subjected to CID fragmentation. Normalized collision energy was set to 35 V and an activation time of 10 ms. Ions in a 10 ppm m/z window around ions selected for MS2 were excluded from further selection for fragmentation for 60 s. The same TOP20 ions were subjected to HCD MS2 event in Orbitrap part of the instrument. The fragment ion isolation width was set to 0.7 m/z, AGC was set to 50,000, the maximum ion time was 200 ms, normalized collision energy was set to 27V and an activation time of 1 ms for each HCD MS2 scan. Raw data were submitted for analysis in Proteome Discoverer 2.1.0.81 (Thermo Fisher) software. Assignment of MS/MS spectra was performed using the Sequest HT algorithm by searching the data against a protein sequence database including all entries from the Human Uniprot database (SwissProt 16,768 and TrEMBL 62,460 total of 79,228 protein forms, 2015) (The UniProt 2017) and other known contaminants such as human keratins and common lab contaminants. Sequest HT searches were performed using a 20 ppm precursor ion tolerance and requiring each peptide's N-/C termini to adhere with Trypsin protease specificity, while allowing up to two missed cleavages. 6-plex tandem mass tags (TMT) on peptide N termini and lysine residues (+229.162932 Da) was set as static modifications while methionine oxidation (+15.99492 Da) was set as variable modification. A MS2 spectra assignment false discovery rate (FDR) of 1% on protein level was achieved by applying the target-decoy database search. Filtering was performed using a Percolator (64bit version (Kall, Storey et al. 2008)). For quantification, a 0.02 m/z window centered on the

theoretical m/z value of each the six reporter ions and the intensity of the signal closest to the theoretical m/z value was recorded. Reporter ion intensities were exported in result file of Proteome Discoverer 2.1 search engine as an excel tables. The total signal intensity across all peptides quantified was summed for each TMT channel, and all intensity values were adjusted to account for potentially uneven TMT labeling and/or sample handling variance for each labeled channel. Candidate proteins were identified as those that had at least 1.5 $\log_2$ fold change between treatment groups.

miRNA inhibitors and lenti-miR viruses: Miridian miRNA hairpin inhibitors directed against mmu-miR-135b-5p or the nonmammalian miRNA cel-miR-67 were obtained from GE Dharmacon (Lafayette, CO). To overexpress (OE) mir-135b-5p, pre-miR-135b-5p or a scramble nontargeting control sequence in the lentiviral vector CD513 were obtained from System Biosciences (Palo Alto, CA). To virally inhibit mir-135b-5p expression, an anti-miR-135b short hairpin (shRNA) that acts as a sponge or scrambled control hairpin cloned into the pGreenPuro shRNA expression lentivector SI505A-1 was purchased from System Biosciences. The OE and shRNA vectors were packaged into lentiviruses using a 2nd generation packaging system at the Emory Viral Vector Core (Emory University, Atlanta, GA). Titers obtained were $1x10^9$ iu/ml for anti-mir, and $3x10^8$ iu/ml for OE.

Intra-amygdalar infusions: miRNA inhibitors, non-targeting controls, or lenti-mirs were injected bilaterally into the BLC (AP: 1.5 mm, ML: ±3.2 mm from bregma and DV: – 4.7 mm from the skull) of mice as previously described (Young, Blouin et al. 2016) using a NanoFil Syringe (World Precision Instruments, Sarasota, FL) that was left in place for 5 minutes after the infusion was complete. Inhibitors were reconstituted in water then prepared with jetPEI transfection reagent (Polyplus Transfection, Illkirch, France). 1ul of 400ng/ul was injected 28 days after fear

conditioning and then animals were tested 48 hours later. For lentiviral experiments, 1.5ul of viruses were injected 23 days after fear conditioning and animals were tested 1 week later to give sufficient time for viral expression.

Dual fluorescence in situ hybridization (FISH): Expression analysis experiments to detect miRNAs were performed as described, with modification (Kasai, Kakihara et al. 2016). Briefly, brains were rapidly removed from anesthetized animals and frozen in isopentane on dry ice. 12um thick sections were cut on a cryostat, dried completely, fixed with 4% formalin, digested with 5ug/ml proteinase K, acetylated and then hybridized at 42°C for 16 hours with LNA dual 5'- and 3'- DIG-labeled probes against mir-135b-5p (TCACATAGGAATGAAAAGCCATA) or a scrambled negative control sequence that was also dual DIG-labeled (Exiqon). Excess probe was removed by saline sodium citrate (SSC) washes at 42°C. For dual detection of hybridized probes, sections were blocked for 1 hour in blocking reagent (Roche, Basel, Switzerland) and then incubated with anti-DIG antibody (1:400, Roche) overnight at 4°C. Sections were washed with TNT buffer then incubated with tyramide signal amplification (TSA) (Perkin Elmer, Waltham, MA) for 10 minutes in the dark to detect the DIG signal with CY3. Sections were mounted with Prolong Gold Diamond antifade mounting media with DAPI (Thermo Fisher) and visualized on an Olympus fluorescent confocal microscope with 60X objective (Tokyo, Japan).

Cell fractionation: Fresh tissue was dissected from naïve animals and immediately placed into homogenization buffer (20mM 4-(2-hydroxyethyl)-1-piperazineethanesulfonic acid [HEPES], 1mM EDTA [pH 7.4], 40U/ul RNASEout [Invitrogen], and Complete phosphatase / protease inhibitors (Roche) as previously described (Most, Ferguson et al. 2015). Tissue was pooled from four animals for each sample and homogenized for 1min with a pestle. To isolate synaptoneurosomes (SN), samples were first spun at 1000g for 2 minutes to remove excess cellular

debris then filtered through a 5um PVDF filter (Millipore). The homogenate was centrifuged at 14,000g for 20 min at 4°C to pellet the cell fraction containing SNs. Proteins were extracted from a small amount of each fraction- total, SN and supernatant containing cytosol and nucleus- to assess the purity of the fractionation by immunoblotting. RNA was extracted from cell fractions with the miRVANA PARIS kit as described above.

Supplementary Text

Fig. S1.

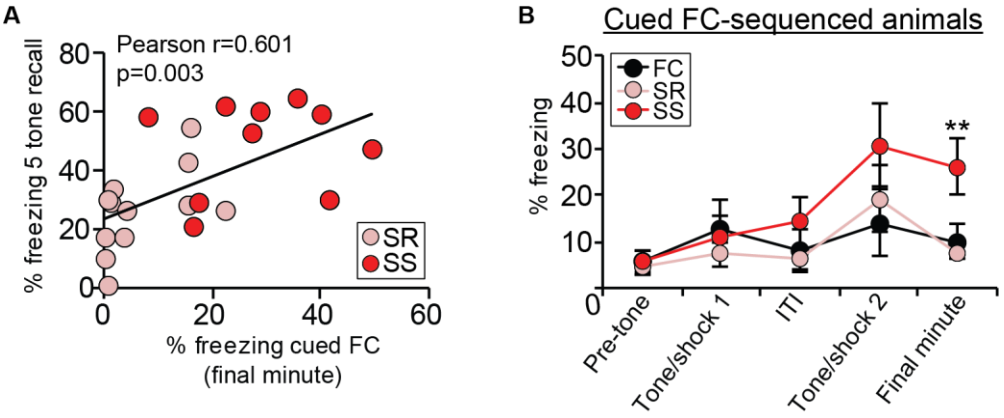

SEFL subgroups can be predicted based on training for molecular analysis.

(A) Pearson correlation between freezing during 5-tone recall test and freezing during cued FC in SEFL trained mice, with animals divided into SR (pink) or SS (red) subgroups based on training. r=0.601; p=0.003 N=22. (B) Cued FC profile of SEFL trained animals used for smRNA-seq (no retrieval). RM-ANOVA between SR and SS: $F_{(1,14)}$ =5.05; p=0.041; post hoc t-test: $t_{(14)}$ =3.315, p=0.0005. N=6-9/group.

Fig S2.

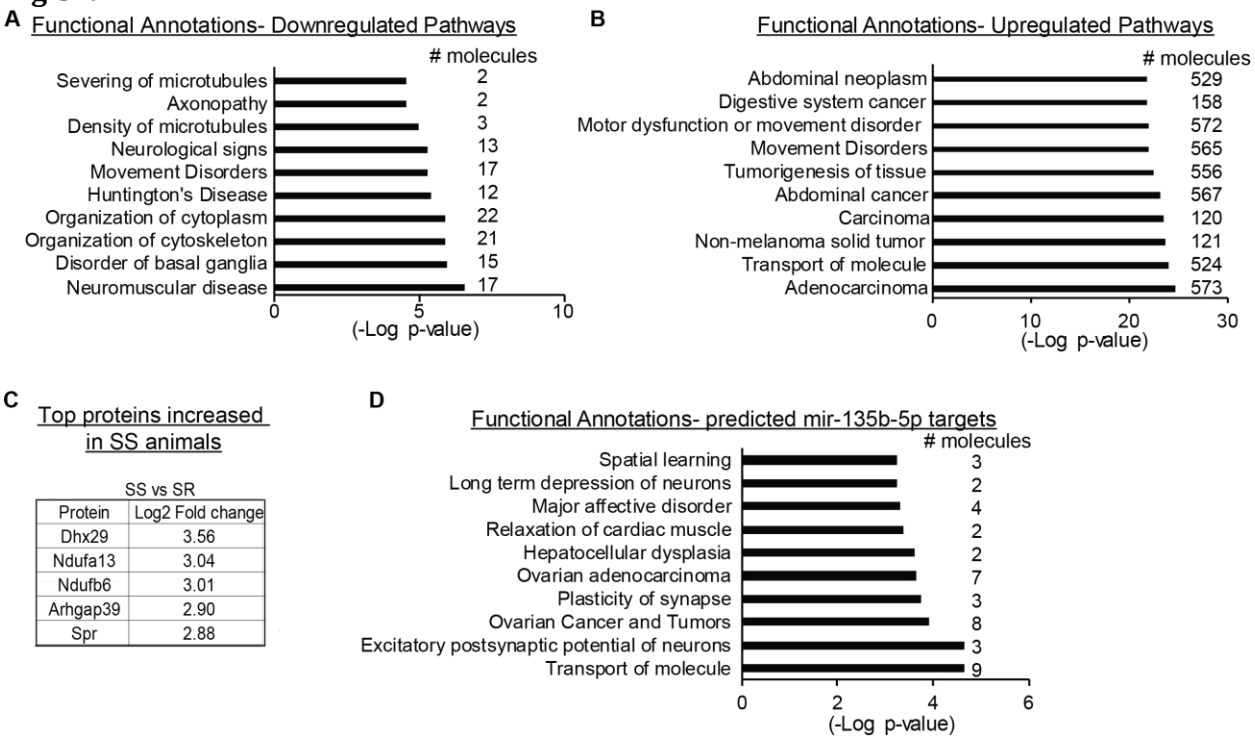

Pathway analysis of mass spec data.

Top 10 significant pathways of downregulated (A) or upregulated proteins (B). (C) The top 5 upregulated proteins in SS vs SR animals identified in the proteomics screen. (D)The top 10 significant pathways of regulated mir-135b-5p target proteins regulated between SS and SR animals.

Fig. S3.

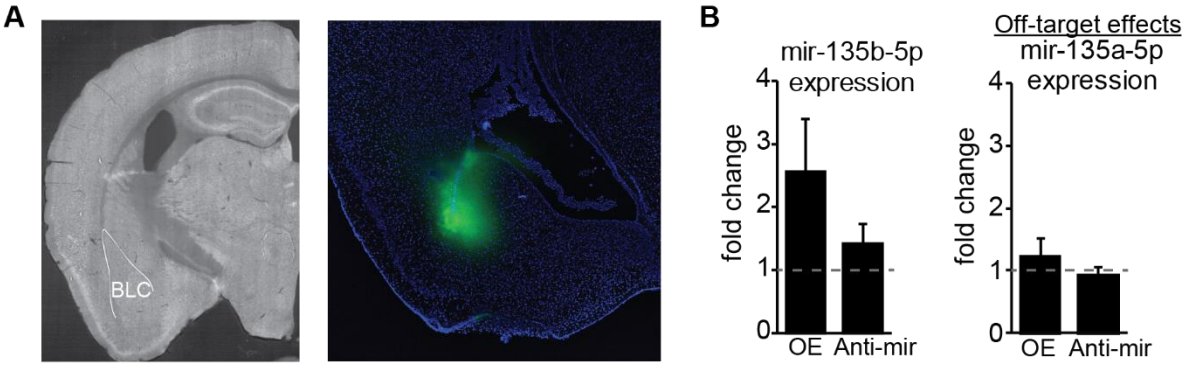

Validation of mir-135b-5p overexpression.

(A) A representative image depicting the location of virus injection into the BLC of adult mice. (B) RNA expression of mir-135b-5p or another mir-135 family member, mir-135a-5p in BLC tissue 7 days after injection of the premirOE-135b-5p virus or anti-mir-135b-5p sponge virus. Expression levels were normalized to tissue injected with viruses containing a non-targeting scrambled sequence.

Fig. S4.

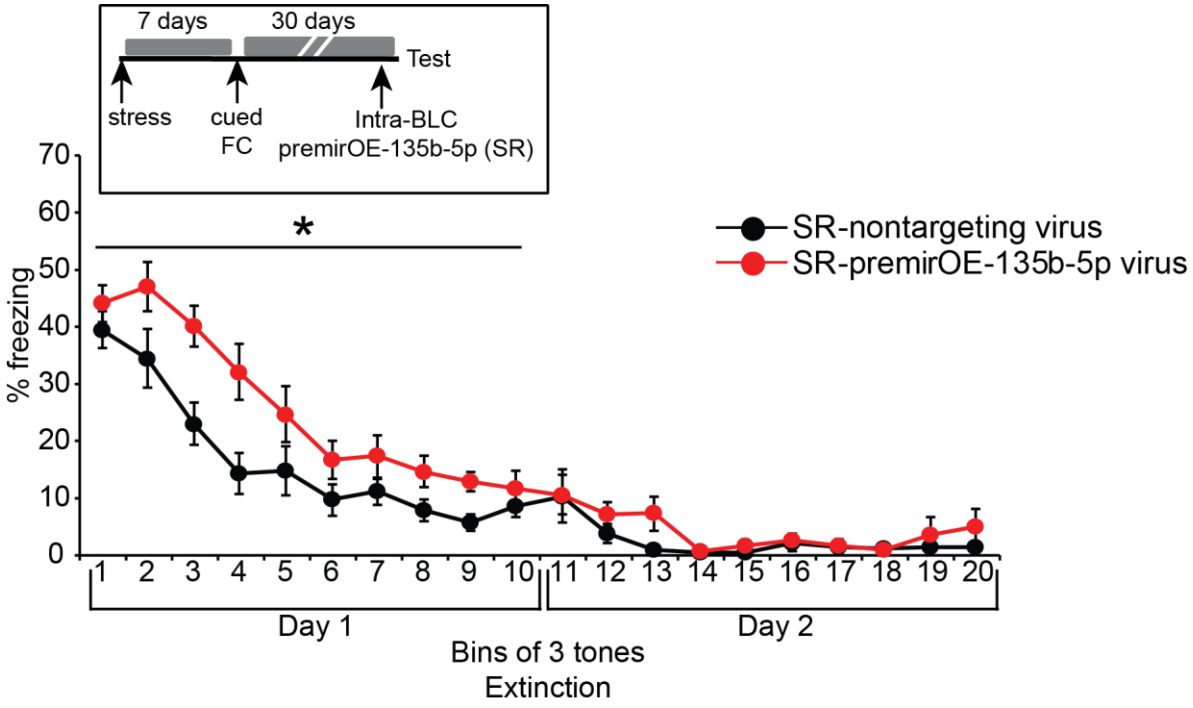

Full extinction curve after mir-135 overexpression in SR mice.

Shown are freezing levels in 3 tone bins for extinction over two days. RM-ANOVA between extinction Day 1: $F_{(1,21)}=6.34$; $p=0.020$. N=10 for SR-nontargeting virus; N=13 for SR-premirOE-135b-5p virus.

Fig. S5.

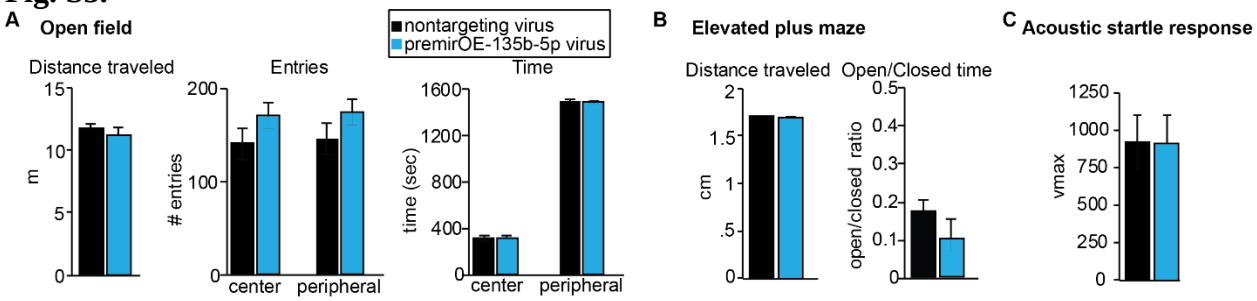

Elevated BLC mir-135b-5p does not affect baseline anxiety levels.

Performance of naïve animals in the open field (A), elevated plus maze (B) and acoustic startle response (C) 7 days after injection with the premirOE-135b-5p virus into the BLC.

Fig. S6.

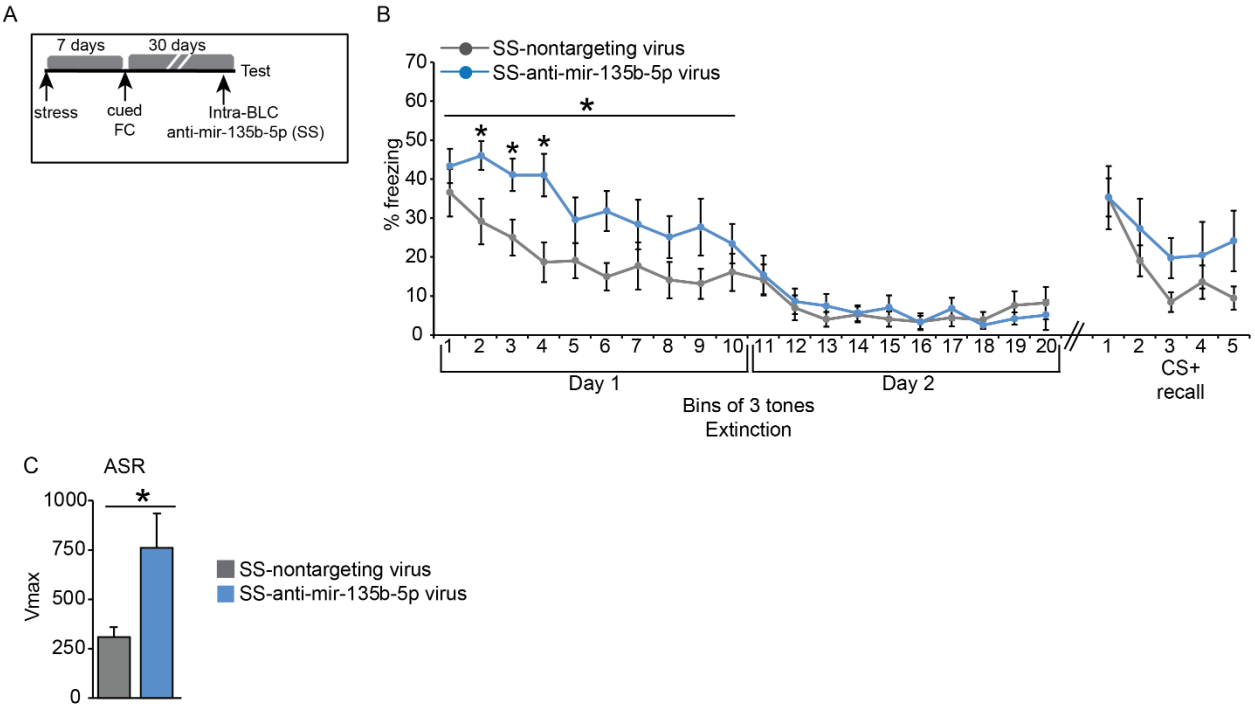

Elevation of mir-135b-5p with anti-mir-135b-5p virus exacerbates the SS phenotype.

(A) High freezing SS animals injected with anti-mir-135b-5p virus 21 days after training were tested for memory strength and extinction resistance 1 week after viral injection. (B) Extinction was performed over two days with 30 tone presentations each day and followed two weeks later with a 5 tone recall test. RM-ANOVA extinction over day 1: $F_{(1,22)}=5.271$; $p=0.032$
Post hoc t-tests: bins 2, 3 and 4, $p<0.05$. N=12 for SS-nontargeting virus; N=12 for SS-anti-mir-135b-5p virus. (C) Prior to the 5-tone recall test, animals were tested in the acoustic startle response (ASR) test for hyperarousal. Unpaired t-test: $t_{(22)}=2.304$, $p=0.0301$. N=12/group.

Fig. S7.

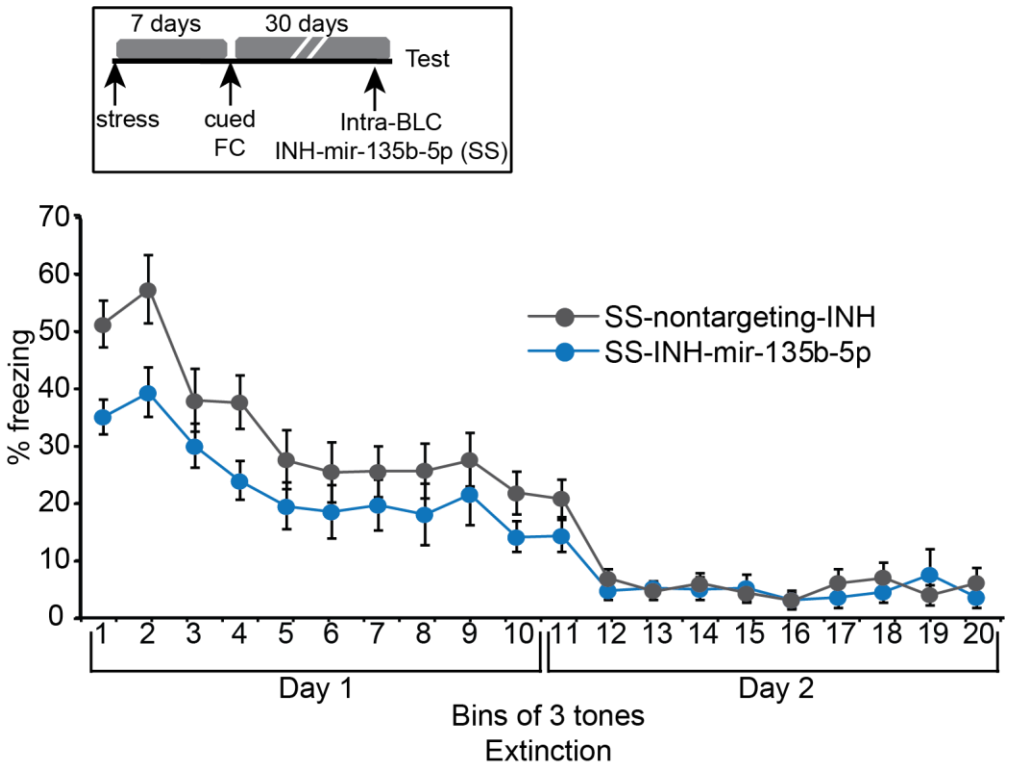

Full extinction curve after mir-135 inhibition in SS mice.

Shown are freezing levels in 3 tone bins for extinction over two days.

Fig. S8.

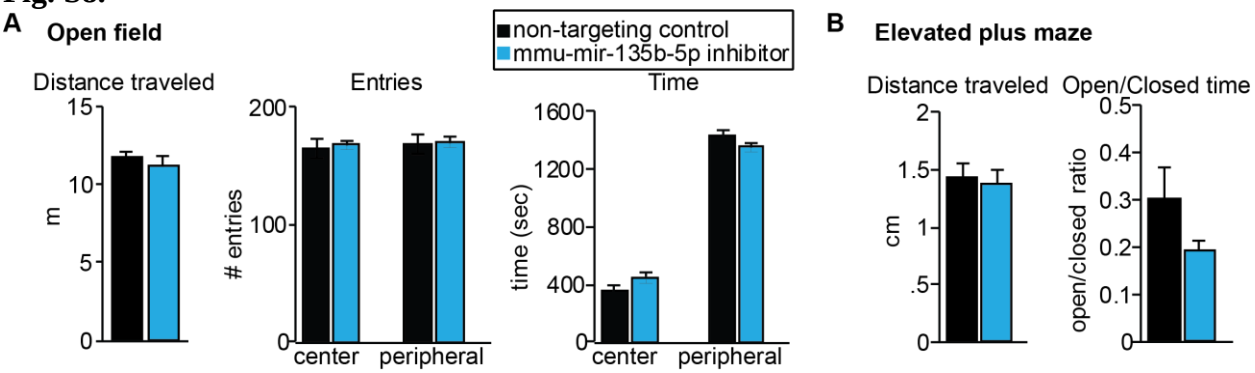

Inhibition of BLC mir-135b-5p tone does not affect baseline anxiety levels.

Performance of naïve animals in the open field (A) and elevated plus maze (B) 2 days after injection with the mir-135b-5p inhibitor into the BLC.

Fig. S9.

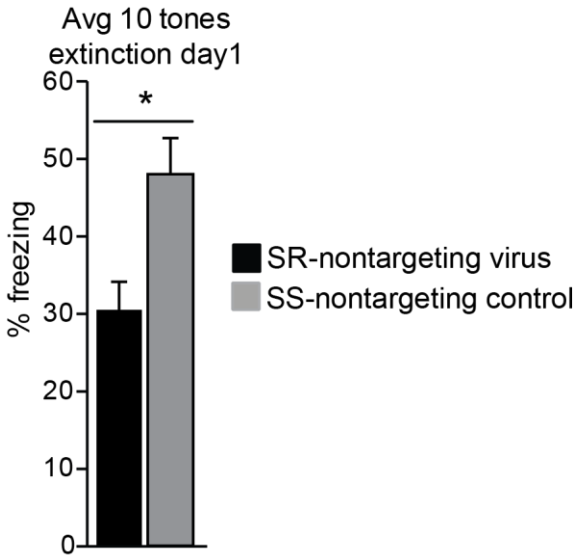

Injection of control miRNA regulating compounds into the BLC does not impact SS or SR phenotypic behavior.

SR and SS animals injected with either a non-targeting control virus (SR) or a nontargeting control inhibitor (SS) were tested during extinction for memory expression. Unpaired t-test: $t_{(22)}$=2.861, p= 0.0091; N=10 (SR), 14 (SS).

Fig. S10

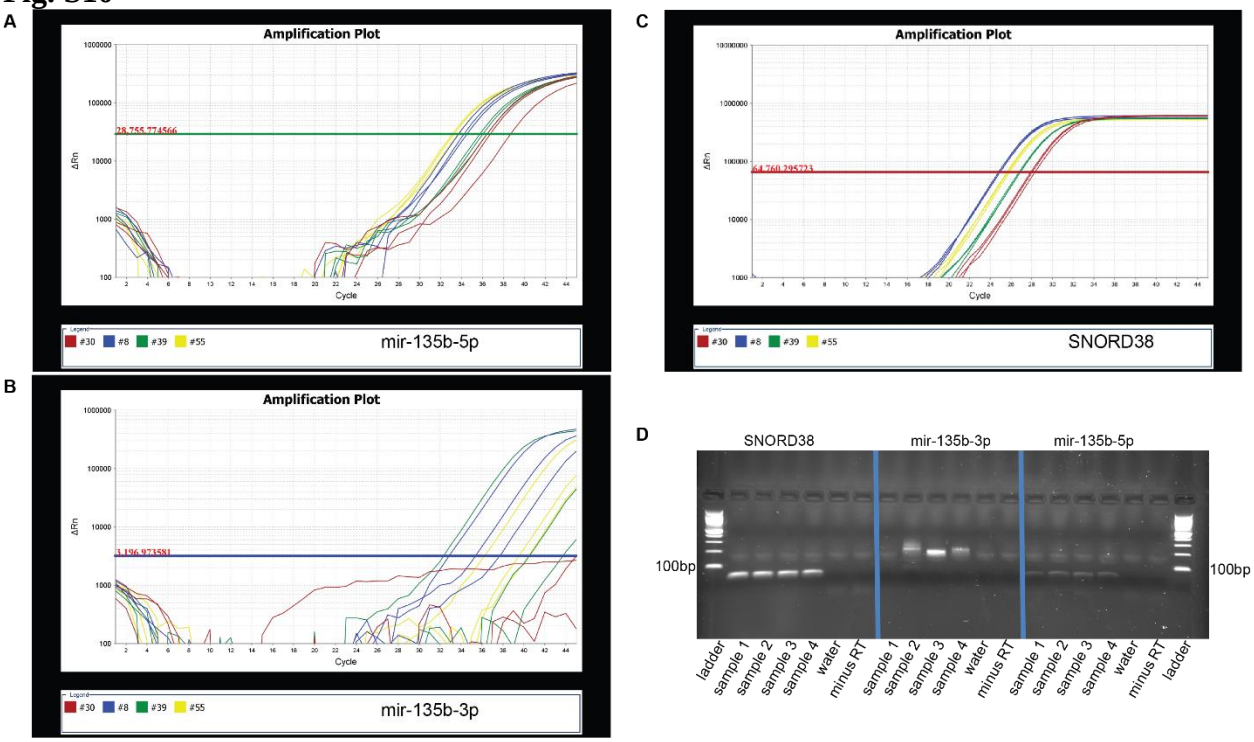

Amplification of mir-135b isoforms in postmortem human amygdala tissue.

(A-C) Amplification plots for mir-135b-5p (A), mir-135b-3p (B) and the housekeeping snoRNA gene SNORD38 (C) obtained by qPCR. (D) Gel electrophoresis analysis of qPCR products.

Table S1.

Supplementary Table 1: List of miRNAs consistently changed between SS and SR animals in both biological replicate sequencing experiments.

		Log2 Fold change	
Gene ID	miRNA name	Run 1	Run 2
MI0000588_2	mmu-miR-103-3p	0.729	0.699
MI0000684_1	mmu-miR-107-3p	1.234	0.922
MI0006298_2	mmu-miR-1193-3p	1.386	0.820
MI0000716_2	mmu-miR-124-3p	1.236	0.567
MI0000150_1	mmu-miR-124-5p	1.014	1.165
MI0004130_2	mmu-miR-1264-3p	1.153	1.118
MI0000585_2	mmu-miR-129-5p	-0.718	-0.529
MI0000715_2	mmu-miR-135a-5p	0.866	0.812
MI0000646_1	mmu-miR-135b-5p	0.539	0.698
MI0000176_2	mmu-miR-154-3p	1.353	1.114
MI0000176_1	mmu-miR-154-5p	0.768	0.752
MI0000687_2	mmu-miR-17-3p	0.792	1.041
MI0000718_2	mmu-miR-19b-3p	1.696	0.509
MI0000709_1	mmu-miR-221-3p	0.810	0.770
MI0000571_2	mmu-miR-23a-3p	0.518	0.525
MI0000394_2	mmu-miR-296-5p	1.375	1.098
MI0000576_1	mmu-miR-29a-3p	1.246	0.968
MI0000576_2	mmu-miR-29a-5p	1.131	0.932
MI0000143_1	mmu-miR-29b-3p	0.525	0.785
MI0000577_2	mmu-miR-29c-3p	1.165	1.619
MI0000817_1	mmu-miR-335-5p	1.235	1.096
MI0000707_1	mmu-miR-33-5p	1.703	1.482
MI0000619_1	mmu-miR-338-3p	1.007	0.656
MI0000621_2	mmu-miR-339-5p	1.002	1.574
MI0000623_1	mmu-miR-340-5p	1.568	0.760
MI0005495_1	mmu-miR-344-3p	1.070	1.090
MI0000632_2	mmu-miR-345-3p	0.511	1.219
MI0000632_1	mmu-miR-345-5p	1.106	0.508
MI0000584_1	mmu-miR-34a-5p	1.161	0.692
MI0000403_2	mmu-miR-34c-5p	0.626	1.741
MI0000763_1	mmu-miR-362-3p	1.666	0.983
MI0000793_2	mmu-miR-376a-3p	0.682	0.883
MI0003533_2	mmu-miR-376c-3p	1.307	1.170
MI0000794_1	mmu-miR-377-5p	0.972	0.759
MI0004639_2	mmu-miR-495-3p	0.713	1.202
MI0004676_1	mmu-miR-499-5p	1.170	0.495

MI0004702_1	mmu-miR-500-3p	1.089	0.640
MI0004131_2	mmu-miR-551b-3p	1.301	0.792
MI0004965_2	mmu-miR-652-3p	0.842	0.625
MI0004684_1	mmu-miR-700-3p	0.633	0.544
MI0000581_1	mmu-miR-93-3p	0.688	0.635
MI0000721_2	mmu-miR-9-3p	1.283	0.923

Table S2.

Supplementary Table 2: Pathway analysis of predicted SS-specific miRNAs from DIANA

KEGG Pathway	microCts	Tarbase	Targetscan
Adherens junction		X	
Allograft rejection			X
Amoebiasis	X		X
Antigen processing and presentation			X
Axon guidance	X		
Biosynthesis of unsaturated fatty acids	X		
ECM-receptor interaction	X	X	X
Endocytosis		X	
Fatty acid biosynthesis		X	
Fatty acid degradation		X	X
Fatty acid metabolism	X	X	X
Focal adhesion	X		
FoxO signaling pathway		X	
GABAergic synapse			X
Glioma	X		
Glycosphingolipid biosynthesis - lacto and neolacto series	X		
Hippo signaling pathway	X	X	
Lysine degradation		X	
Metabolic pathways		X	
Morphine addiction			X
Mucin type O-Glycan biosynthesis	X		X
PI3K-Akt signaling pathway	X		
Prion diseases		X	
Protein digestion and absorption	X		X
Proteoglycans in cancer		X	
Signaling pathways regulating pluripotency of stem cells	X		
Steroid biosynthesis		X	
Thyroid hormone signaling pathway	X	X	

.